J|A|C|S
ARTICLES
Published on Web 07/13/2006

Theoretical Characterization of Cyclic Thiolated Gold Clusters

Henrik Grönbeck,[†,*] Michael Walter,[‡] and Hannu Häkkinen[‡]

Contribution from the Department of Applied Physics and Competence Centre for Catalysis, Chalmers University of Technology, SE-412 96 Göteborg, Sweden, and Nanoscience Center and Department of Physics FI-40014 University of Jyväskylä, Finland

Received April 20, 2006; E-mail: ghj@chalmers.se

Abstract: The density functional theory is used to explore structural, energetic, vibrational, and optical properties of thiolated gold clusters $(MeSAu)_x$ with $x = 2-12$. Clusters up to $(MeSAu)_4$ adopt Au−S ring conformations, and crownlike structures are formed for larger sizes. The clusters are essentially polymeric and show convergence in structural and energetic properties at $(MeSAu)_4$. The nature of the Au−S bond is polar covalent with a degree of cyclic electron delocalization. Vibrational analysis reveals characteristic Au−S stretch vibrations at ∼300 cm^{-1}. Effects of ligand substitution are studied in the case of the tetramer by comparing the results for methylthiolate with hexylthiolate, benzenethiolate, and glutathionate (GS). The choice of ligand has clear effects on electronic properties. For example, the optical gap is ∼1.5 eV lower for $(GSAu)_4$ than for $(MeSAu)_4$.

I. Introduction

Functionalization of gold is often realized via ligands with sulfur acting as a headgroup (RS). One example is self-assembled monolayers (SAMs) of disulfides or *n*-alkanethiolates on extended gold surfaces[1,2] which have potential applications as biocompatible materials, in lithography, and as chemical sensors. Sulfur ligands are key components also in the rapidly growing field of protected gold nanoparticles (AuNP).[3,4] Such systems can be produced with a narrow and controlled size distribution by reduction of a metal salt in the presence of thiols[5] and possess, in particular, interesting optical and charging properties.

A prerequisite for the stability of SAMs on gold surfaces or AuNPs is the strong RS−Au bond. Due to the buried interface, it has been difficult to experimentally establish fundamental issues such as the stable adsorption configuration of the headgroup. Although thiols often are assumed to be adsorbed as thiolates, intact thiol adsorption has also been reported.[6,7] For SAMs grown on Au(111) the proposed structures include RS−SR dimers[8] or thiolates in atop configurations.[9] Definite structural determinations for thiolate protected AuNP are still missing. The experimental uncertainty has stimulated several theoretical investigations. Early reports with cluster models of Au(111)[10] have been followed by studies of thiol, thiolate, and disulfide adsorption on extended (111) surfaces,[11−14] nanoclusters,[15−17] and small clusters.[18−20] The combined effort has revealed that adsorption as thiolates is favored over disulfides and that thiol dissociation into thiolate and atomic hydrogen may be stabilized by subsequent H_2 formation. On Au(111), thiolates are predicted to adsorb in three-fold hollow,[11,13] hollow-bridge,[14] or bridge configurations.[12] The situation is partly different on nanoclusters and clusters, where the stable adsorption site is bridge or atop. Although the RS−Au interaction is dependent on system size, the calculations agree on the bond as being strong with polar covalent character. For low dimensional systems, the RS−Au interaction is of similar strength as that of the metal−metal cohesion. As a consequence, Au−Au bonds are predicted to break prior to the Au−S contact upon mechanical stress.[21]

Gold complexes of the homoleptic type $(RSAu)_x$ (completely thiolated Au clusters) are a molecular analogue to SAMs on extended surfaces or thiolate protected Au nanoparticles.

[†] Chalmers University of Technology.
[‡] University of Jyväskylä.

(1) Nuzzo, R. G.; Allara, D. L. *J. Am. Chem. Soc.* **1983**, *105*, 4481.
(2) Ulman, A. *Chem. Rev.* **1996**, *96*, 1533.
(3) Schmid, G. *Clusters and Colloids*; VCH: Weinheim, Germany, 1994.
(4) Daniel, M. C.; Astruc, D. *Chem. Rev.* **2004**, *104*, 293.
(5) Brust, M.; Walker, M.; Bethell, D.; Schiffrin, D. J.; Whyman, R. J. *J. Chem. Soc., Chem. Commun.* **1994**, p 801.
(6) Nuzzo, R. G.; Zegarski, B. R.; Dubois, L. H. *J. Am. Chem. Soc.* **1987**, *109*, 733.
(7) Hasan, M.; Bethell, D.; Brust, M. *J. Am. Chem. Soc.* **2001**, *124*, 1132.
(8) Fenter, P.; Schreiber, F.; Berman, L.; Scoles, G.; Eisenberger, P.; Bedzyk, M. J. *Surf. Sci.* **1998**, *412/413*, 213.
(9) Shimada, T.; Kondoh, H.; Nakai, I.; Nagasaka, M.; Yokota, R.; Ohta, K. A. T. *Chem. Phys. Lett.* **2005**, *406*, 232.
(10) Sellers, H.; Ulman, A.; Shnidman, Y.; Eilers, J. E. *J. Am. Chem. Soc.* **1993**, *115*, 9389.
(11) Grönbeck, H.; Curioni, A.; Andreoni, W. *J. Am. Chem. Soc.* **2000**, *122*, 3839.
(12) Vargas, M. C.; Giannozzi, P.; Selloni, A.; Scoles, G. *J. Phys. Chem. B* **2001**, *105*, 9509.
(13) Yourdshahyan, Y.; Zhang, H. K.; Rappe, A. M. *Phys. Rev. B* **2001**, *63*, 081405.
(14) Gottschalck, J.; Hammer, B. *J. Chem. Phys.* **2002**, *116*, 784.
(15) Häkkinen, H.; Barnett, R. N.; Landman, U. *Phys. Rev. Lett.* **1999**, *82*, 3264.
(16) Curioni, A.; Andreoni, W.; Grönbeck, H. *Int. J. Quantum Chem.* **2000**, *80*, 598.
(17) Garzon, I. L.; Rovira, C.; Michaelian, K.; Beltran, M. R.; Ordejon, P.; Junquera, J.; Sanchez-Portal, D.; Artacho, E.; Soler, J. M. *Phys. Rev. Lett.* **2000**, *85*, 5250.
(18) Fuchs, H.; Kruger, D.; Rousseau, R.; Marx, D.; Parrinello, M. *J. Chem. Phys.* **2001**, *115*, 4776.
(19) Konopka, M.; Rousseau, R.; Stich, I.; Marx, D. *J. Am. Chem. Soc.* **2004**, *126*, 12103.
(20) Letardi, S.; Cleri, F. *J. Chem. Phys.* **2004**, *120*, 10062.
(21) Kruger, D.; Fuchs, H.; Rousseau, R.; Marx, D.; Parrinello, M. *Phys. Rev. Lett.* **2002**, *89*, 186402.

10.1021/ja062584w CCC: $33.50

Interestingly, there is growing evidence for the relevance of $(RSAu)_x$ in the area of AuNP. Au(I)−thiolate complexes have been suggested to act as precursors for AuNP formation,[22−24] and recently, $Au_{10}(SG)_{10}$, $Au_{11}(SG)_{11}$, and $Au_{12}(SG)_{12}$ were observed as the smallest components upon reduction of $HAuCl_4$ by $NaBH_4$ in the presence of glutathion (GSH).[25] In fact, $(RSAu)_x$ units may also be relevant for the understanding of ligand exchange reactions. Very recent DFT-based calculations suggest that $(RSAu)_4$ units play a crucial role in the protection of gold nanoparticles and are instrumental in providing an explanation to ligand-exchange reactions that involve a change of the gold nuclearity.[26] Experimentally, it has been observed that the size of the metal cores increases when phosphines are replaced by thiolates[27−29] and decreases during the reversed reaction.[30]

Metal−thiolate complexes have been the subject of several experimental investigations.[31] As thiolates preferably adsorb in bridge configurations, it is often assumed that metal(I)−thiolate complexes adopt zigzag structures forming rings or strands.[31,32] However, few structures have been experimentally confirmed. Structural determinations using X-ray crystallography are difficult due to poor crystal quality, and measurements in solutions are hampered by poor solubility.[24] However, ringlike structures have been reported for complexes with four, five, and six gold atoms. $Au_4[SC(SiMe_3)]_4$ is one such example.[33] This compound has a square structure with Au in a linear coordination and S atoms in the corners. Novel catenane structures have been reported for $[Au(SC_6H_4\text{-}p\text{-}CMe_3)]_{10}$ and $[Au(SC_6H_4\text{-}o\text{-}CMe_3)]_{12}$, which consist of five- and six-membered Au rings, respectively.[34] A cyclic configuration has also been determined for $[AuSC_{15}H_{23}]_6$, revealing a closed chairlike Au−S framework.[35] Some gold complexes are used as therapeutic agents,[32] and the antiarthritic drug gold thiomalate (myochrysine) has been reported to have a structure of a Au−S double helix.[36] Theoretically, efforts on Au(I) complexes have been directed toward small linear compounds[37−41] and the importance of Au−Au auriophilicity for complex clustering.[39,41]

Given the growing evidence for the importance of homoleptic thiolate complexes in the chemistry of thiolate protected gold nanoclusters, and the lack of systematic characterization of such systems, we have performed extensive density functional theory (DFT) calculations for $(MeSAu)_x$, with $x = 2-12$, where Me is a methyl group (CH_3). The clusters are characterized with respect to structural, electronic, vibrational, and optical properties. To explore ligand effects, the results for $(MeSAu)_4$ are compared with calculations where Me is replaced by hexylthiolate (SC_6H_{13}), benzenetiolate (SC_6H_5), and glutathionate ($SC_{10}O_6N_3H_{16}$).

II. Computational Approach

The calculations are performed within the pseudopotential plane-wave (PP-PW) implementation of the density functional theory (DFT).[42,43] In particular, the CPMD code is used[44−47] for the major part of the calculations. The calculations apply the gradient corrected approximation to the exchange-correlation functional according to Perdew, Burke, and Ernzerhof (PBE).[48] Previous comparisons show that this functional provides a fair compromise for the description of both the metal and the organic ligands.[11]

Norm conserving angular dependent pseudopotentials are used to describe the interaction between the valence electrons and the atomic cores.[49] The potentials are derived from solutions to the all-electron (in the case of Au relativistic) Kohn−Sham equation. To be consistent with the exchange-correlation functional used in the calculations, the potentials are generated with the PBE functional. The following core radii were used in the construction of the pseudopotentials (Å): Gold s(1.23), p(1.23), d(0.78); sulfur spd(0.79); carbon sp(0.63); and oxygen sp(0.63). For hydrogen, an analytical local potential is used. The one-electron orbitals are expanded in plane waves up to a kinetic energy of 55 Ry. Structures are considered converged when the largest gradient is smaller than 0.0005 Ha/a_0.

The finite systems are calculated in a cubic embedding geometry with decoupled periodic images.[50,51] All systems are treated in the lowest spin states, namely singlets for $(RSAu)_x$ and doublets for the radicals (RS) and the Au atom.

The optical spectra are evaluated within the linear-response time-dependent DFT (TD-DFT) formalism[52] that was implemented and tested in refs 53, 54. This set of calculations is done with the Born−Oppenheimer Molecular Dynamics (BO-MD) implementation[50] of DFT. In brief, the weights F_I and energies $\hbar\omega_I$ of optical transitions I are obtained by solving the eigenvalue problem $\Omega F_I = \omega_I^2 F_I$. The matrix elements of Ω contain a diagonal term that gives the energy difference of Kohn−Sham (KS) single-particle energies and a nondiagonal term that mixes the KS particle-hole transition (ij) with (kl). The convergence of the spectra depends on the extent of the particle-hole basis and on the size of the grid representing the wave functions. The results presented here use ∼2000 particle-hole transitions and are converged up to ∼4.5 eV.

III. Results and Discussion

A. Structure and Stability of Cyclic $(MeSAu)_x$. We explored homoleptic $(MeSAu)_x$ structures based on cyclic motifs. For each cluster size, a large number of structural configurations were relaxed to a local minimum. For the largest system, $(MeSAu)_{12}$, additional searches were performed to find low

(22) Hostetler, M. J.; Wingate, J. E.; Zhong, C. J.; Harris, J. E.; Vachet, R. W.; Clark, M. R.; Londono, J. D.; Green, S. J.; Stokes, J. J.; Wignall, G. D.; Glish, G. L.; Porter, M. D.; Evans, N. D.; Murray, R. W. *Langmuir* **1998**, *14*, 17.
(23) Chen, S.; Templeton, A. C.; Murray, R. W. *Langmuir* **2000**, *16*, 3543.
(24) Corbierre, M. K.; Lennox, R. B. *Chem. Mater.* **2005**, *17*, 5691.
(25) Negishi, Y.; Nobusada, K.; Tsukuda, T. *J. Am. Chem. Soc.* **2005**, *127*, 5261.
(26) Häkkinen, H.; Walter, M.; Grönbeck, H. *J. Phys. Chem. B* **2006**, *120*, 9927.
(27) Woehrle, G. H.; Brown, L. O.; Hutchison, J. E. *J. Am. Chem. Soc.* **2005**, *127*, 2172.
(28) Balasubramanian, R.; Guo, R.; Mills, A. J.; Murray, R. W. *J. Am. Chem. Soc.* **2005**, *127*, 8126.
(29) Shichibu, Y.; Negishi, Y.; Tsukuda, T.; Teranishi, T. *J. Am. Chem. Soc.* **2005**, *127*, 13464.
(30) Wang, W.; Murray, R. W. *Langmuir* **2005**, *21*, 7015.
(31) Dance, I. G. *Polyhedron* **1986**, *5*, 1037.
(32) Shaw, C. F. *Chem. Rev.* **1999**, *99*, 2589.
(33) Bonasia, P. J.; Gindelberger, D. E.; Arnold, J. *Inorg. Chem.* **1993**, *32*, 5126.
(34) Wiseman, M. R.; Marsh, P. A.; Bishop, P. T.; Brisdon, B. J.; Mahon, M. F. *J. Am. Chem. Soc.* **2000**, *122*, 12598.
(35) LeBlanc, D. J.; Lock, C. J. L. *Acta Crystallogr.* **1997**, *C53*, 1765.
(36) Bau, R. *J. Am. Chem. Soc.* **1998**, *120*, 9380.
(37) Häberlen, O. D.; Rösch, N. *J. Phys. Chem.* **1993**, *97*, 4970.
(38) Pyykkö, P.; Li, J.; Runeberg, N. *Chem. Phys. Lett.* **1994**, *218*, 133.
(39) Schmidbaur, H. *Chem. Soc. Rev.* **1995**, p 391.
(40) Pyykkö, P.; Runeberg, N.; Mendizabal, F. *Chem. Eur. J.* **1997**, *3*, 1451.
(41) Pyykkö, P. *Chem. Rev.* **1997**, *97*, 597.
(42) Hohenberg, P.; Kohn, W. *Phys. Rev.* **1964**, *136*, 864.
(43) Kohn, W.; Sham, L. J. *Phys. Rev.* **1965**, *140*, A1133.
(44) Car, R.; Parrinello, M. *Phys. Rev. Lett.* **1985**, *55*, 2471.
(45) CPMD v3.9; Copyright IBM Corp 1990−2001, Copyright MPI fuer Festkoerperforschung Stuttgart 1997−2001.
(46) Marx, D.; Hutter, J. *Modern Methods and Algorithms in Quantum Chemistry*; Forschungzentrum Juelich NIC Series, 2000; Vol. 1.
(47) Andreoni, W.; Curioni, A. *Parallel Computing* **2000**, *26*, 819.
(48) Perdew, J.; Burke, K.; Ernzerhof, M. *Phys. Rev. Lett.* **1996**, *77*, 3865.
(49) Troullier, N.; Martins, J. L. *Phys. Rev. B* **1991**, *43*, 1993.
(50) Barnett, R. N.; Landman, U. *Phys. Rev. B* **1993**, *48*, 2081.
(51) Hockney, R. W. *Methods Comput. Phys.* **1970**, *9*, 136.
(52) Casida, M. E. *Modern Methods and Algorithms in Quantum Chemistry*; Seminario, J. M., Ed.; Elsevier: Amsterdam, 1996.
(53) Moseler, M.; Häkkinen, H.; Landman, U. *Phys. Rev. Lett.* **2001**, *87*, 053401.
(54) Walter, M.; Häkkinen, H. *Phys. Rev. B* **2005**, *72*, 205440.

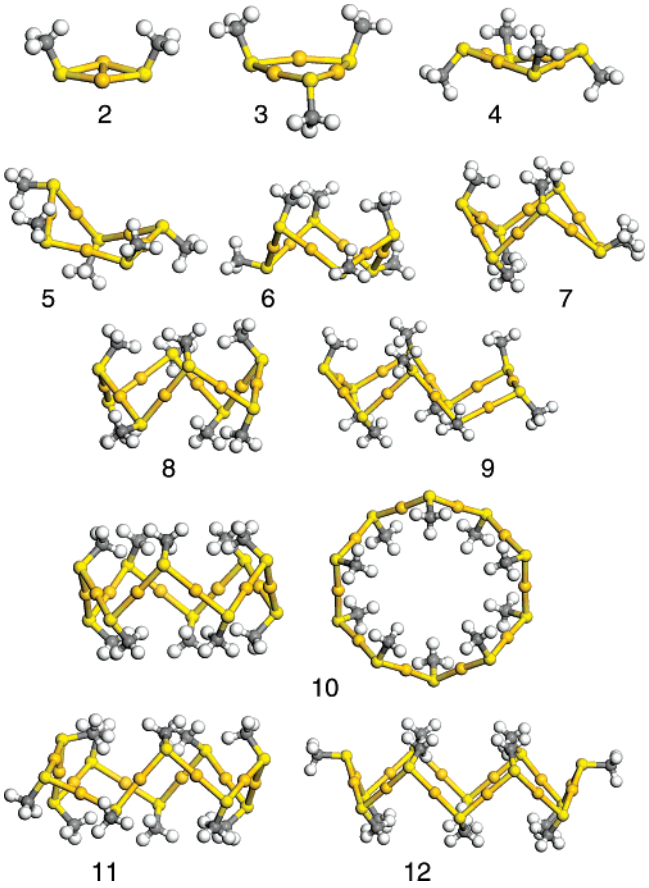

Figure 1. Optimized ring configurations for $(MeSAu)_x$. Color code: orange (Au), yellow (S), gray (C), and white (H).

energy isomers based on a thiolate capped gold core. However, all such structures were considerably higher in energy than the one presented below. One should note that bare gold clusters in the studied size regime tend to be planar.[55−58] Thus, for these small clusters, the thermodynamic drive toward formation of compact three-dimensional structures is small.

The lowest energy structures for $(MeSAu)_x$, $x = 2-12$, are shown in Figure 1. To make the structural motif clear, two views of $(MeSAu)_{10}$ are displayed. In all cases, the methyl thiolates are bonded in bridge configurations, building up closed rings or crowns. An open configuration was investigated for $(MeSAu)_4$ and found to be 2.53 eV higher in energy than the isomer reported in Figure 1. This energy is similar to the MeS−Au bond strength in the monomer, which is calculated to be 2.46 eV.

For $(MeSAu)_2$, a cis-like isomer is favored over a trans-isomer by 0.04 eV. This is the only size, where the methyl groups prefer the same orientation with respect to the Au−S network. For $(MeSAu)_3$, one methyl group is oriented differently as compared to the other two. The cis-isomer is higher in energy by 0.03 eV. $(MeSAu)_4$ in the trans-conformation is preferred by 0.10 eV over the cis-geometry. For $(MeSAu)_2$ to $(MeSAu)_4$, the Au−S frameworks are close to planar. For the larger sizes, the directionality in the S bonds develops a zigzag motif. The first case is $(MeSAu)_5$, which forms a bent structure. For $(MeSAu)_6$, the lowest energy isomer is a chair conformation with three of the methyl groups pointing away from the center of the ring. However, the isomer with the groups arranged in a regular "up−down" fashion is only 0.03 eV higher in energy. As the size of the cyclic structure increases, the characteristic zigzag motif becomes clearer. All even low energy isomers have the Au atoms in a plane. This is in part a consequence of the zigzag pattern; however, as will be discussed below, direct Au−Au interactions further stabilize such conformations.

As an even number of MeSAu units allow for a regular zigzag pattern, the even clusters obey a somewhat higher structural order. In this sense, odd clusters have to accommodate a "structural defect". The higher symmetry of the even clusters is, in particular, evident for $(MeSAu_3)_{10}$ that adopts a circular structure with a symmetric "up−down" arrangement of the methyl groups. For all cluster sizes, numerous possibilities exist as to the orientation of the S−C bond with respect to the plane defined by the neighboring Au−S−Au bonds, and several isomers are energetically degenerate. However, spontaneous isomerization was not observed in short (∼2 ps) Car−Parrinello[44] molecular dynamics simulations for $(MeSAu)_4$ and $(MeSAu)_6$. It is clear that longer or branched ligands could introduce a larger degree of inter-ligand order.

It is not surprising that stoichiometric thiolated gold clusters adopt a zigzag pattern. It is a consequence of the propensity for the linear coordination geometry of Au(I) complexes[39] in conjugation with the double bridging character of thiolate ligands.[31] One may note that a zigzag motif is also relevant for bare sulfur clusters, where the crown-shaped structure of cyclo-octasulfur (S_8) is the best known example. In ref 59, sulfur clusters (S_2) to (S_{13}) were investigated within the local density approximation of DFT. In fact, for (S_3) to (S_8), the low energy isomers coincide with the arrangement of the sulfur atoms in $(MeSAu)_x$ shown in Figure 1. In similarity with $(MeSAu)_x$, the structural flexibility for S_x clusters is large, where several isomers compete for the ground state.[59] We note that although the zigzag motif is established for metal−thiolate structures,[31] clear observations of such structures for Au complexes are rare.[34,35]

The key parameters in the structural characterization of the thiolated Au clusters are collected in Table 1. The data reveal

Table 1. Structural Parameters for the Lowest Energy Isomers of $(MeSAu)_x$[a]

	d_{Au-S}	d_{S-C}	d_{Au-Au}	$\alpha_{Au-S-Au}$	α_{S-Au-S}
$(MeSAu)_2$	2.50	1.83	2.76	67.1	112.6
$(MeSAu)_3$	2.38	1.84	3.02	78.7	161.0
$(MeSAu)_4$	2.34	1.84	3.32	90.2	177.5
$(MeSAu)_5$	2.34	1.84	3.43	94.4	177.9
$(MeSAu)_6$	2.34	1.84	3.36	91.8	177.6
$(MeSAu)_7$	2.34	1.84	3.35	92.8	177.1
$(MeSAu)_8$	2.34	1.84	3.33	90.5	178.0
$(MeSAu)_9$	2.34	1.84	3.44	94.6	177.6
$(MeSAu)_{10}$	2.34	1.84	3.37	92.0	176.7
$(MeSAu)_{11}$	2.34	1.84	3.42	94.5	176.8
$(MeSAu)_{12}$	2.34	1.84	3.40	93.3	177.1

[a] d_{Au-S}, d_{Au-Au}, and d_{S-C} are the mean Au−S, Au−Au, and S−C bond distances (Å), respectively. $\alpha_{Au-S-Au}$ and α_{S-Au-S} are the Au−S−Au and S−Au−S angles, respectively.

(55) Häkkinen, H.; Moseler, M.; Landman, U. *Phys. Rev. Lett.* **2002**, *89*, 033401.
(56) Furche, F.; Ahlrichs, R.; Weis, P.; Jacob, C.; Gilb, S.; Bierweiler, T.; Kappes, M. *J. Chem. Phys.* **2002**, *117*, 6982.
(57) Yoon, B.; Häkkinen, H.; Landman, U.; Li, X.; Zhai, H. J.; Wang, L. S. *J. Phys. Chem. A* **2003**, *107*, 6168.
(58) Grönbeck, H.; Broqvist, P. *Phys. Rev. B* **2005**, *71*, 073408.
(59) Hohl, D.; Jones, R. O.; Car, R.; Parrinello, M. *J. Chem. Phys.* **1988**, *89*, 6823.

Table 2. Stability of $(MeSAu)_x$ Rings (eV)[a]

	E_{mf}	E_f
$(MeSAu)_2$	1.16	0.58
$(MeSAu)_3$	4.07	1.74
$(MeSAu)_4$	1.96	1.96
$(MeSAu)_5$	1.97	1.97
$(MeSAu)_6$	2.01	1.98
$(MeSAu)_7$	1.96	1.98
$(MeSAu)_8$	2.01	1.98
$(MeSAu)_9$	1.96	1.97
$(MeSAu)_{10}$	2.03	1.98
$(MeSAu)_{11}$	1.96	1.97
$(MeSAu)_{12}$	2.05	1.99

[a] The fragmentation energy per MeSAu unit is denoted E_f, whereas the monomer fragmentation energy is denoted E_{mf}.

a rapid convergence. Already for $(MeSAu)_4$, the distances and angles are close to the values calculated for the largest systems investigated.

The calculated structures compare well with available experimental data on gold complexes with other ligands. In ref 33, among various compounds, $(AuSC(SiMe_3))_4$ was prepared, crystallized, and characterized with X-ray crystallography. The mean Au−S distance, Au−S−Au angle, and S−Au−S angle were reported to be 2.30 Å, 91.9°, and 177.5°, respectively. A cyclic hexamer $(AuSC_{15}H_{23})_6$ was prepared, and the crystal was structurally characterized in ref 35. For this compound, the average Au−S and S−C distances were reported to be 2.29 and 1.80 Å, respectively; the Au−S−Au angle was reported to be 102°, and the S−Au−S angle, to be 175°. Although the measurements are performed on crystals, the slightly expanded theoretical Au−S distance as compared to the experiments could be attributed to the approximation used for the exchange-correlation as elaborated on in ref 11.

The stability of the $(MeSAu)_x$ low energy isomers is reported in Table 2. The monomer fragmentation energy (E_{mf}) is calculated as $E_{mf} = E[(MeSAu)_{x-1}] + E[MeSAu] - E[(MeSAu)_x]$, and the fragmentation energy per MeSAu unit (E_f), as $E_f = (xE[MeSAu] - E[(MeSAu)_x]/x$. Similar to the structural properties, the energetic stability converges fast. Already the tetramer could be regarded as converged. The minor difference between the fragmentation energy and the monomer fragmentation energy signals that the clusters (with exception of the dimer and trimer) essentially are polymeric. The stabilities show a small but clear odd−even alternation. The even clusters are somewhat more stable than the odd. This is related to the possibility of even clusters adopting a more regular zigzag pattern. In fact, also the standard deviation of the S−Au−S and Au−S−Au angles for the low energy isomers obey an odd−even pattern (not shown) with a smaller deviation for the even clusters than for the adjacent odd clusters.

The cohesion of rings should be related to other relevant bond strengths in the system: the MeS−Au bond strength and the Au−Au cohesion. The strength of the MeS−Au bond is calculated to be 2.46 eV for the monomer. Reoptimizing the bare Au_4[60] and Au_{12}[57] clusters within the present computational scheme yields a cohesion (Au-atom fragmentation) energy of 1.47 (2.42) eV for Au_4 and 2.04 (2.82) eV for Au_{12}. Thus, in the investigated size range, the metal−metal cohesion is smaller or in the same range as the MeSAu−MeSAu cohesion in the thiolated clusters. This suggests that small thiolated gold clusters

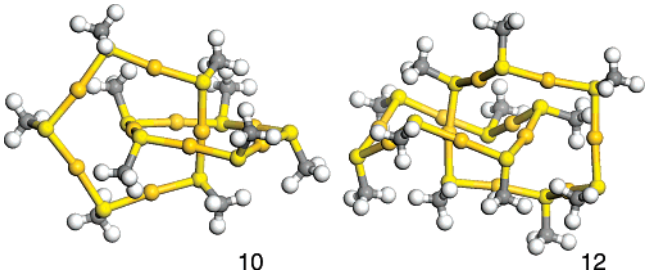

Figure 2. Catenane structures for $(MeSAu)_{10}$ and $(MeSAu)_{12}$. See Figure 1 for color code.

should prefer open cyclic structures instead of a compact metal core structure capped by a protecting thiolate layer. A consequence of this energy balance for AuNP was recently explored using $Au_{38}(SCH_3)_{24}$ as an example.[26] A novel open O_h symmetry structure was found with six $(MeSAu)_4$ rings protecting the central Au core. Consequently, this cluster could be characterized as $Au_{14}[(MeSAu)_4]_6$.

B. Structure and Stability of $(MeSAu)_x$ Catenanes. In addition to structures based on a monocyclic motif, two catenane isomers were considered for $(MeSAu)_{10}$ and $(MeSAu)_{12}$. Such conformations with interlocked pentamer and hexamer rings, respectively, have been experimentally observed with other ligands.[34] In ref 34, $(AuSC_6H_4$-*p*-$CMe_3)_{10}$ and $(AuSC_6H_4$-*o*-$CMe_3)_{12}$ were prepared and structurally characterized. It was found that the two pentamers or hexamers interpenetrate with one Au atom of one ring situated close to the center of the other ring.

The structural results for catenane conformations of $(MeSAu)_{10}$ and $(MeSAu)_{12}$ are shown in Figure 2.[61] For $(MeSAu)_{10}$, the two pentamer rings are close to planar. Thus, the ring−ring interaction counteracts some of the bent structure present for the single pentamer geometry (see Figure 1). For the catenane structure, there are two Au−S distances. The Au−S distance involving the Au atom at the center of the ring is 2.40 Å, whereas other Au−S distances are ∼2.35 Å, which is close to the values in Table 1. The decamer complex in ref 34 comprised two close to planar pentamer units and two distinctly different Au−S bond lengths, namely 2.34 Å for bonds involving the center atom and 2.28 Å for the rest. Hence, although different ligands were used in ref 34, the two systems are in qualitative agreement.

The hexamer units in the catenane structure of $(MeSAu)_{12}$ are nonplanar, following the zigzag pattern of the isolated units. For this conformation, the Au−S distances involving the center Au atom is 2.36 Å, whereas other Au−S distances are ∼2.35 Å. In ref 34, $(AuSC_6H_4$-*o*-$CMe_3)_{12}$ was measured to consist of buckled hexamers and Au−S separations in the range 2.29−2.32 Å, with no appreciable difference for the Au−S distances for Au atoms making the ring−ring contact. Again, the theoretical results are in accordance with the experimental data.

The catenane conformations are energetically slightly preferred with respect to the corresponding single ring structures. For $(MeSAu)_{10}$, the catenane structure is 0.16 eV below the monocrown, whereas the corresponding value is 0.29 eV for $(MeSAu)_{12}$. The two rings are bonded by 0.23 and 0.28 eV for

(60) Grönbeck, H.; Andreoni, W. *Chem. Phys.* **2000**, *262*, 1.

(61) A catenane structure for $(MeSAu)_8$ based on $(MeSAu)_4$ rings was not stable. It relaxed into a Au−S network at 0.8 eV higher energy than the stable cyclic $(MeSAu)_8$ isomer. Structures with rings of mixed sizes for odd $(MeSAu)_x$ clusters were not considered.

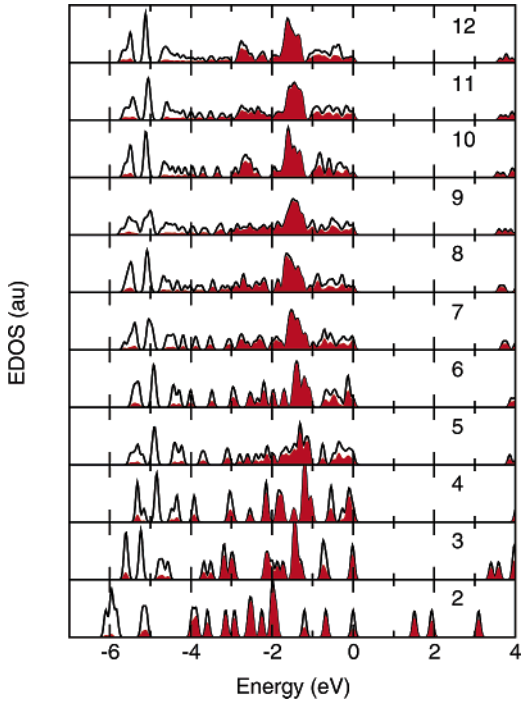

Figure 3. Electronic density of states (EDOS) for the low energy isomers. The energies are reported with respect to the corresponding HOMO level, which is at zero level. The shaded areas correspond to the projection on Au orbitals. The one-electron Kohn−Sham energies have been broadened with a 0.1-eV Gaussian.

$(MeSAu)_{10}$ and $(MeSAu)_{12}$, respectively. This is within the energy range of typical "aurophilic" Au−Au interactions.[39,41] However, as the present form of DFT does not include dispersion interactions, this agreement could be accidental. As will be discussed below, the Au−Au contact has a pronounced effect in the electronic structure of these systems.

C. Electronic Properties. The electronic density of states (EDOS) for the low energy isomers of the ring structures are reported in Figure 3. The EDOS has been obtained by a 0.1-eV Gaussian broadening of the one-electron Kohn−Sham energy levels. For comparison, each EDOS has been normalized by the number of MeSAu units in the cluster. The EDOS reveals that these systems are "molecular" in the sense that all sizes have large HOMO−LUMO gaps.[62] The smallest gap (1.5 eV) is calculated for the dimer. The trimer has a gap of 3.4 eV, and the largest gap for the studied systems is predicted for the tetramer which is 4 eV. The gap appears to reach a converged value of ∼3.6 eV for $(MeSAu)_7$.

The shaded part of the spectra in Figure 3 is the partial density of states (PDOS) corresponding to Au states. The PDOS is calculated by projection of the one-electron Kohn−Sham orbitals onto the atomic Au pseudoorbitals. The remaining weight of the DOS in the reported energy interval is mainly of sulfur character, although some C and H contributions are present. The occupied PDOS shows two types of Au states. States of pure Au character are centered ∼1.75 eV below the HOMO level and correspond to Au *d* orbitals. States of mixed Au−S character are present both below and above the pure Au states.

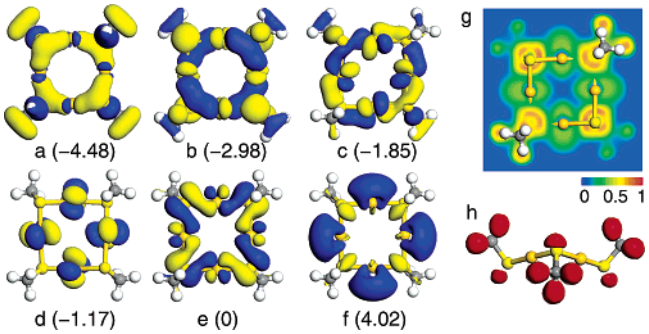

Figure 4. (a−f) Selected Kohn−Sham orbitals for $(MeSAu)_4$ are shown. (e) The corresponding energy (eV) relative to the HOMO is indicated. (f) The LUMO. The iso-surfaces are depicted at a value of ±0.025 au. (g) The contour of the ELF through the plane defined by the Au atoms, and (h) the ELF iso-surface for a value of 0.9. See Figure 1 for color code of the atoms.

Some representative examples of Kohn−Sham orbitals for $(MeSAu)_4$ are shown in Figure 4. In Figure 4, the energy relative to the HOMO level is indicated. Orbital (a) is mainly located on the methylthiolates, but a clear hybridization with Au *d* orbitals is present which forms a closed cyclic pattern. For (b), the weights on the Au atoms are larger, and the cyclic character of the orbital is even more pronounced. *s* and *d* orbital aromaticity has recently been discussed for cyclo-$Au_3L_nH_{3-n}$ with $n = 1-3$ and L = Me as one example.[63] The electron delocalization in ref 63 was originating from direct Au−Au interactions. For orbitals (a) and (b) of $(MeSAu)_4$, the sulfur *p* orbitals contribute to the delocalization by hybridization with gold *d* orbitals. The Kohn−Sham orbital (d) is a pure Au *d* state with the atomic orbitals in phase. At the chosen iso-value, the signs of direct contact are only weakly indicated. However, such direct Au−Au contacts probably favor structural configurations with the Au atoms in a plane. Orbital (c) and the HOMO level (e) are clear examples of Au(*d*)−S(*p*) hybridization, giving the bond a covalent nature. The LUMO level (f) is of Au character with both 6*s* and 6*p* contributions.

To further analyze the Au−S bond, the electron localization function (ELF)[64] was evaluated, and the result for $(MeSAu)_4$ is reported in Figure 4. For the ELF, a value of $^1/_2$ corresponds to an electron gas, whereas a value of 1 corresponds to perfect localization. The slice through the Au atoms indicates that the Au electrons are delocalized and that localization is present around the S atom. The iso-surface at 0.9 shows the high electron localization near hydrogen atoms and the presence of a lone pair on sulfur. The lone pair is a signature of sp^3 hybridization for sulfur. To conclude, the Au−S bond in the cyclic structures is covalent in nature but with novel elements of electron delocalization. Furthermore, there is a clear polarization of the interaction in the clusters. A Mulliken analysis yields a Au charging of about +0.4 electrons per atom.

In Figure 5, the EDOS for the investigated $(MeSAu)_{10}$ catenane structure is shown. Interestingly, this EDOS is clearly different from those for the spectra of $(MeSAu)_5$ and $(MeSAu)_{10}$ in Figure 3. Two states have appeared in the "gap", reducing the HOMO−LUMO separation to 2.5 eV. The two states are located 0.5 and 1.0 eV above the manifold of occupied states, respectively. The gap between the manifold of occupied and

(62) HOMO: Highest Occupied Molecular Orbital. LUMO: Lowest Unoccupied Molecular Orbital.

(63) Tsipis, A. C.; Tsipis, C. A. *J. Am. Chem. Soc.* **2005**, *127*, 10623.
(64) Becke, A. D.; Edgecombe, K. E. *J. Chem. Phys.* **1990**, *92*, 5397.

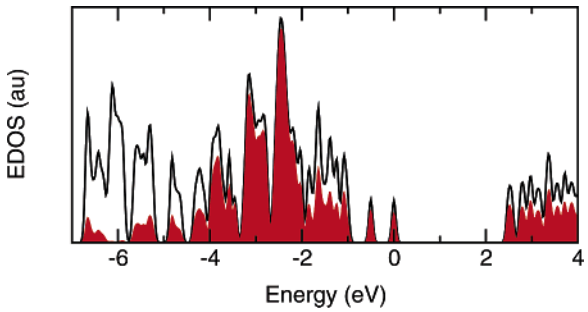

Figure 5. Electronic density of states (EDOS) for the $(MeSAu)_{10}$ catenane structure. The shaded areas correspond to the projection on Au orbitals. The one-electron Kohn−Sham energies have been broadened with a 0.1-eV Gaussian.

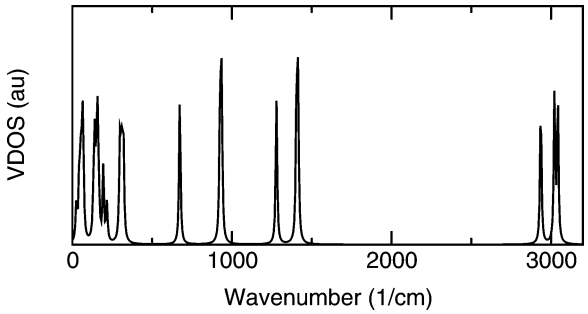

Figure 6. Vibrational density of states for $(MeSAu)_4$.

unoccupied states is 3.7 eV. This is similar to the gap for the larger monocyclic structures. The two states in the gap are a signature of the Au−Au contact in the catenane isomer and are of pure Au character. Inspection of the Kohn−Sham orbitals reveals that they correspond to a bonding and an antibonding combination of Au orbitals on the two contact atoms, respectively. The situation is similar for the catenane structure of $(MeSAu)_{12}$ compared to that of $(MeSAu)_{10}$. However, in this case the two states are located only 0.25 and 0.5 eV above the manifold of occupied states, respectively.

D. Vibrational Analysis of $(MeSAu)_4$. Vibrational spectroscopy is a powerful technique for investigating bonding properties. This technique was, for example, recently applied to gold nanoparticles protected by benzenethiolates.[65] In Figure 6, the result of a vibrational analysis of $(MeSAu)_4$ is reported. The vibrational density of states (VDOS) is obtained by a 5-cm^{-1} Lorentzian broadening of the calculated eigenmodes.

The different bonds in the system clearly correspond to different vibrational wavenumbers. The high wavenumbers, centered at ∼3000 cm^{-1}, are C−H stretch vibrations. The vibrations at 1410, 1280, and 930 cm^{-1} are also related to the methyl group, corresponding to the scissors, umbrella, and waving modes, respectively. The S−C stretch vibrations appear at 670 cm^{-1}. Owing to the polar character of the bond, the Au−S stretch vibration should be IR-active. These modes appear in a band centered at ∼300 cm^{-1}. The modes at lower wavenumbers are Me−S wiggles (∼150 cm^{-1}), and the softest modes below 100 cm^{-1} are modes of the Au−S framework.

As a consequence of the polymeric nature of the bonding in $(MeSAu)_x$ with $x > 4$, one could assume that the vibrational spectrum does not change appreciably for the larger sizes. This was verified by explicit calculations for $(MeSAu)_6$ and $(MeSAu)_{10}$.

(65) Price, R. C.; Whetten, R. L. *J. Am. Chem. Soc.* **2005**, *127*, 13750.

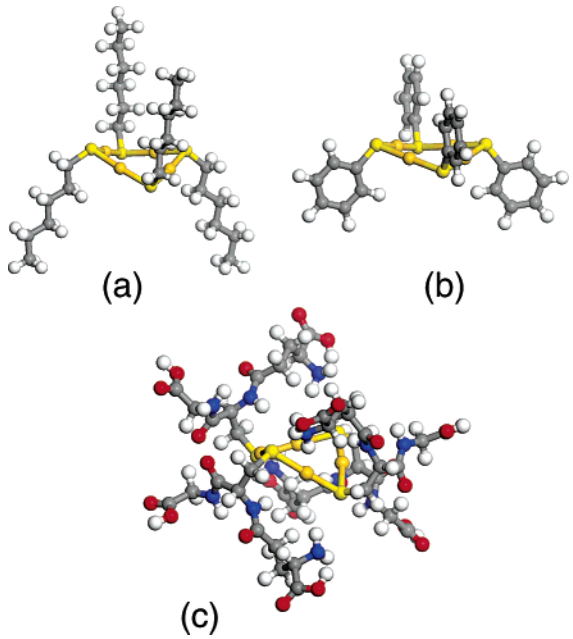

Figure 7. Optimized structures for $(RSAu)_4$ with SR being (a) hexylthiolate, (b) benzenethiolate, and (d) glutathionate. Color code: orange (Au), yellow (S), red (O), blue (N), gray (C), and white (H).

E. Effects of Ligands for $(RSAu)_4$. Most theoretical studies on the interaction of thiols and thiolates with gold surfaces, nanoparticles, and clusters have been conducted with short ligands, which in the case of alkylthiolates corresponds to methylthiolates. The use of such short ligands is based on the fact that the Au−S interaction is assumed to be insensitive to the length of the carbon chain. In fact, this appears to be a fair approximation.[18] In ref 18 a similar computational approach as the present one was used to compare methylthiolate adsorption with ethylthiolate and propylthiolate adsorption on Au_1−Au_4. The Au−S bond strength variation was in all cases within 0.07 eV.

However, most experiments on thiolate protected gold systems are performed with other ligands than methylthiolate. Generally, the shortest alkyl chain used in experiments is hexyl. Moreover, other types of ligands than alkyls are frequently used including glutathionate[25,29] and benzenethiolate.[65] In the present study, the role of the ligand is explored by comparing the results for $(MeSAu)_4$ with $(RSAu)_4$, where SR = $-SC_6H_{13}$ (hexylthiolate), $-SC_6H_5$ (benzenethiolate), and ($-SC_{10}O_6N_3H_{16}$) (glutathionate, −SG).

The optimized low energy isomers are shown in Figure 7. In agreement with $(MeSAu)_4$, the lowest energy isomers correspond to a trans-configuration. For the bulky glutathionate, this was the only considered conformation. The cis-structure was 0.05 (0.15) eV higher in energy than the trans-geometry for benzenethiolate (hexylthiolate). For hexylthiolate, an additional structure resembling an SAM was considered. However, this isomer was 0.32 eV higher in energy than the favored geometry in Figure 7.

Some of the structural parameters are compared with those of $(MeSAu)_4$ in Table 3. The results show that the structure of the Au−S framework depends weakly on the choice of ligand. The Au−S distances are in all cases close to 2.35 Å. Naturally, the S−C distance is a more sensitive measure of the ligand. Whereas the distances for the methylthiolate and hexylthiolate

Table 3. Structural Parameters for $(RSAu)_4$ with Different Ligands[a]

	d_{Au-S}	d_{S-C}	d_{Au-Au}	$\alpha_{Au-S-Au}$	α_{S-Au-S}
$(CH_3SAu)_4$	2.34	1.84	3.32	90.2	177.5
$(C_6H_{13}SAu)_4$	2.35	1.85	3.31	89.4	175.2
$(C_6H_5SAu)_4$	2.35	1.80	3.29	89.0	178.7
$(GSAu)_4$	2.35	1.86	3.24	86.8	172.6

[a] Same notations as those in Table 1.

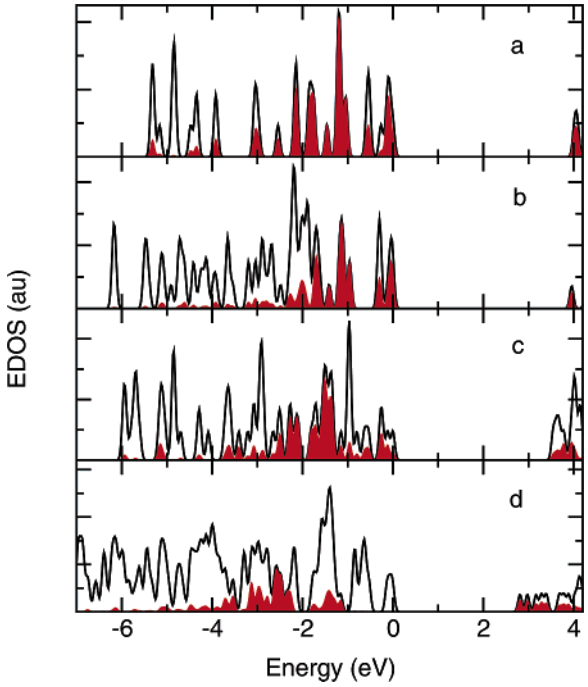

Figure 8. Electronic density of states (EDOS) for $(RSAu)_4$ with SR being (a) methylthiolate, (b) hexylthiolate, (c) benzenethiolate, and (d) glutathionate. The shaded areas correspond to the projection on Au orbitals. The one-electron Kohn−Sham energies have been broadened with a 0.1-eV Gaussian.

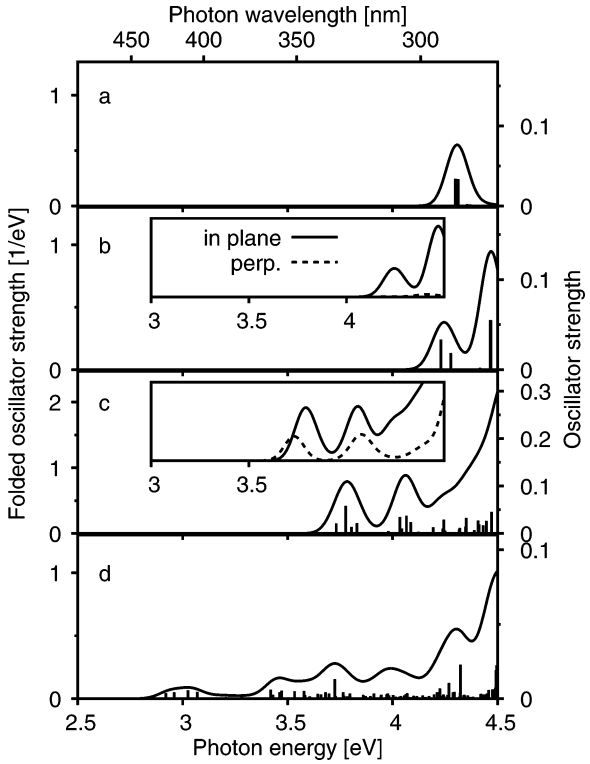

Figure 9. Absorption spectra for $(RSAu)_4$ with SR being (a) methylthiolate, (b) hexylthiolate, (c) benzenethiolate, and (d) glutathionate. Polarization resolved spectra (see text) are shown as insets for hexylthiolate and benzenethiolate. The folded oscillator strength is obtained by a broadening of each transition by a 0.05-eV Gaussian.

are similar, the S−C distance for the benzenethiolate is considerably shorter. For glutathionate, the distance is close to the result for the alkyl chains. The Au−Au distances as well as the angles show some effects on the choice of ligand. However, as discussed above, the framework vibrations are soft, and the differences could also result from direct ligand−ligand interactions. In particular, the bulky SGs have the smallest angles and shortest Au−Au distances.

The stability of $(RSAu)_4$ shows a weak dependence on ligand. The fragmentation energy is calculated to be 1.96 eV, 1.96 eV, 1.86, and 1.93 eV for methylthiolate, hexylthiolate, benzenethiolate, and glutathionate, respectively. This is consistent with the changes in the structural parameters near the Au−S bond and the systematic study in ref 18 on alkylthiolates.

The electronic densities of states for $(RSAu)_4$ with different ligands are displayed in Figure 8. The results for $(CH_3SAu)_4$ and $(C_6H_{13}SAu)_4$ are similar. The HOMO−LUMO gap is in both cases close to 4 eV. A smaller gap (3.5 eV) is present for $(C_6H_5SAu)_4$. Both the HOMO and LUMO have in this case a larger degree of ligand contribution as compared to the alkylthiolates. The smallest gap is predicted for $(GSAu)_4$. In this case, the Au character of the HOMO is missing. Instead, this state is localized at the oxygen atoms in the ligands. Overall, the EDOS for the different systems shows the presence of states with pure Au characteristics and a substantial Au−S hybridization.

Thus, even though the structural and energetic changes for $(RSAu)_4$ upon ligand exchange are minor, the electronic structure is clearly dependent on the ligand. This has important implications for probes of the electronic spectrum, such as photoabsorption.

F. Optical Photoabsorption. The interest in optical properties of Au nanoparticles has been considerable.[4] Here, the TD-DFT formalism is applied to explore the optical response for the different $(RSAu)_x$ systems. The absorption spectrum is studied with respect to the (i) choice of ligand, (ii) size and shape of the cyclic conformation, and (iii) presence of Au−Au contacts for catenane structures.

The effect of ligand on optical spectra is investigated by calculating the spectrum of $(RSAu)_4$ where R is methylthiolate, hexylthiolate, benzenethiolate, and glutathionate. The results for the near-UV range is shown in Figure 9. The optical gaps (∼4.2 eV) are similar for the two systems with alkylthiolates. A marked reduction of the gap is predicted for the cluster protected by benzenethiolates, and with glutathionates the gap is ∼2.7 eV, implying a reduction of 1.5 eV with respect to $(MeSAu)_4$. The general trend is in agreement with the Kohn−Sham EDOS reported in Figure 8. With the exception of glutathionate, the optical gap is ∼0.2 eV larger than the corresponding HOMO−LUMO separation. For $(GSAu)_4$, the optical and HOMO−LUMO gaps coincide. Because TD-DFT transitions consist of several interfering particle-hole transitions, a transparent analysis is cumbersome. However, more information on the nature of

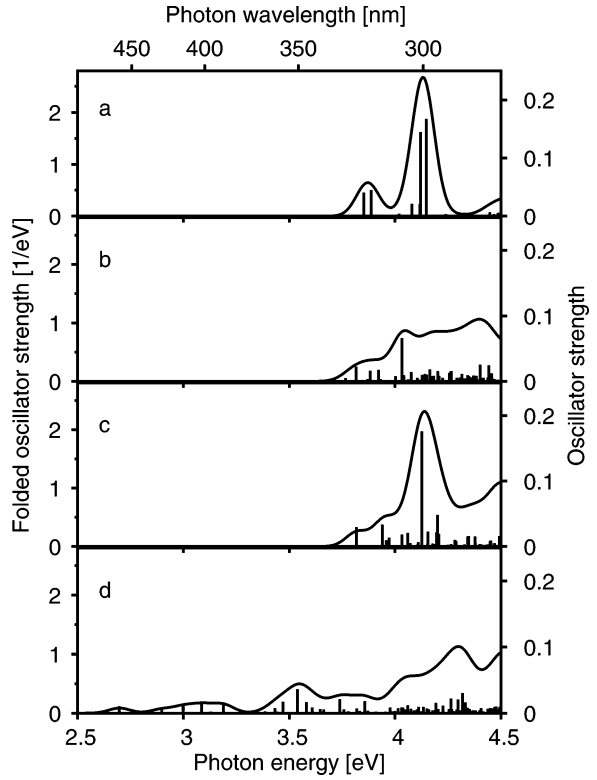

Figure 10. Absorption spectra of $(MeSAu)_x$ with an (a) $x = 10$ monocyclic crown, (b) $x = 11$ monocyclic crown, (c) $x = 12$ monocyclic crown, and (d) $x = 10$ catenane conformation. The folded oscillator strength is obtained by a broadening of each transition by a 0.05-eV Gaussian.

the transitions can be gained by analyzing the polarization resolved spectra.[54] The resolved spectra for the hexylthiolate and benzenethiolate are shown as insets in Figure 9. The hexylthiolate protected cluster is excited only by light polarized in the plane formed by the Au atoms. The absorption for light polarized perpendicular to this plane (the main direction of the hexyl groups) is very weak. This clearly indicates that the transitions in this energy interval are connected to states in the Au−S framework. In the case of benzenethiolate ligands, the strongest absorption is observed also in the direction of the plane formed by the Au atoms. However, a clear component of the oscillator strength is calculated for light polarized perpendicular to the Au−S frame, indicating transitions involving the ligands.

In contrast to the other complexes, $(GSAu)_4$ shows a fairly close agreement between the TD-DFT spectrum and the (unscreened) Kohn−Sham transition probabilities (not reported) in the region up to ∼3.5 eV. Inspection of the Kohn−Sham states contributing to these transitions reveals that the transitions originate from excitations of electronic states in the ligand to empty states near or in the Au−S framework. In ref 25 the absorption spectrum for a mixture of $(GSAu)_{10}$, $(GSAu)_{11}$, and $(GSAu)_{12}$ was measured in an aqueous solution. In particular, the optical gap was determined to be 2.9 eV. Effects of the solution as well as the difference in system size could certainly influence the picture; however, we note the similarity with the onset of the absorption predicted here (2.7 eV) for $(GSAu)_4$.

To exemplify the effect of system size, conformation, and Au−Au contacts on absorption spectra, the results for $(MeSAu)_x$ for $x = 10-12$ are shown in Figure 10. The optical gaps for these systems are considerably lower than that for $(MeSAu)_4$. For the monocyclic systems, the gap is ∼3.8 eV. The optical gap appears to be converged with respect to the cluster size for the $x = 10-12$. This is actually also what the results for the Kohn−Sham EDOS (Figure 3) suggest. The peaked absorption spectra for $(MeSAu)_{10}$ and $(MeSAu)_{12}$ are a consequence of the high structural symmetry for these systems. The low symmetry of the odd cluster $(MeSAu)_{11}$ results in a featureless absorption profile.

As compared to the monocyclic structures, the catenane form of $(MeSAu)_{10}$ has a considerably lower optical gap (2.6 eV). This correlates with the Kohn−Sham EDOS (Figure 5). Owing to the low symmetry of this system, the peak structure is weak.

The optical absorption spectrum of $[Au_{13}(SCH_3)_8]^{3+}$ was recently investigated within TD-DFT using an implementation of DFT based on local basis functions.[66] In ref 66, the structural search was restricted to the O_h molecular symmetry, yielding an octahedral Au−S framework and a central Au atom. The calculated spectrum had an onset at ∼2.3 eV. The difference in chemical composition and the high charge state, as well as the constrained structure in ref 66, make a comparison with the present results difficult.

IV. Conclusions

There is growing evidence for the importance of homoleptic $(RSAu)_x$ complexes within the field of thiolate protected Au nanoparticles. The present work represents the first systematic theoretical characterization of such systems. Using methylthiolate as a model ligand, a structural search was performed in the size range $x = 2-12$. Planar Au−S ring structures are predicted for $x = 2-4$, whereas the larger sizes adopt crownlike zigzag strands. The systems are essentially polymeric, showing a convergence in stability and electronic properties for $(MeSAu)_4$. Vibrational analysis reveals characteristic Au−S stretch vibrations at ∼300 cm^{-1}.

Effects of different ligand types were investigated for $(RSAu)_4$ comparing results for methylthiolate with hexylthiolate, benzenethiolate, and glutathionate. The structural effects in the Au−S framework were found to be minor. However, the HOMO−LUMO separation for benzenethiolate and, in particular, glutathionate was considerably reduced as compared with the results for the alkylthiolates. This fact has important implications for the optical photoabsorption properties of the systems. The optical gap for $(GSAu)_4$ was calculated to be ∼1.5 eV lower than the corresponding gap for $(MeSAu)_4$.

Acknowledgment. CPU time granted at PDC (Stockholm, Sweden) and CSC (Espoo, Finland) is gratefully acknowledged. The Competence Centre for Catalysis is hosted by Chalmers University of Technology and financially supported by the Swedish Energy Agency and the member companies AB Volvo, Volvo Car Corporation, Scania CV AB, GM Powertrain Sweden AB, Haldor Topsoe A/S, Perstorp Specialty Chemicals AB, and The Swedish Space Agency. The work was partially supported by the Academy of Finland (M.W. and H.H.).

JA062584W

(66) Nobusada, K. *J. Phys. Chem. B* **2004**, *108*, 11904.